Waterflood-CMG production optimization analysis for the Draugen field of Norway

Tendai Zisengwe[1], Bruce Mutume*[2]

[1] Department of Petroleum and Natural Gas Engineering, Near East University, North Cyprus.

[2] Sustainable Environment and Energy Systems department, Middle East Technical University, North Cyprus.

[*] Corresponding author, Email: bruce.mutume@metu.edu.tr

Abstract

The Draugen field is well-known for producing oil that is then transported to power plant facilities to generate electricity in Draugen. However, with declining oil production (as of 2021) and new necessary electrification contracts, the field may be unable to meet the demand for plant facilities. The current study combines waterflooding and reservoir simulation methods from the Computer Modelling Group (CMG) to evaluate the effectiveness of the secondary recovery type of production optimization. The approach is divided into three parts to meet the current study's objectives: (1) matching reservoir dimensions (Draugen's and the model's dimensions) to match Draugen field's Original Oil in Place (OOIP), (2) history matching, and (3) production optimization analysis using CMG. The estimated recoverable oil before the waterflood-CMG optimization analysis (in 2021) was 99 500 000 m^3, but after optimization (2050), the recoverable oil increased to 108 370 000 m^3. The waterflood method increased the drawdown by 250 times that of the simulation's start, increasing the production rate from 0 to over 1 500 m^3/day/well. Finally, the former resulted in the recovery of 8 8700 000 m^3 of oil, proving the viability of the secondary type recovery method at the Draugen field. Consequently, the oil saturation decreased from a high of 35 to 60 % to the field's residual oil saturation range of 21 to 23 %. Our results support the adoption of the waterflooding technique for oil optimization at Draugen field.

Keywords: Waterflooding, Oil optimization, Oil production, Reservoir simulation, Draugen field

Introduction

Optimization refers to a mathematical formula in which an algorithm is used to compute a set of values of decision variables that minimizes or maximizes a constrained objective function [1]. So, in the oil and gas industry, it is a way of modifying and improving a well's/field's previous traditional completion and production modes and parameters [2]. Different methods must be implemented for each reservoir when pressure begins to fall during oil or gas production. Few of the world's wells flow naturally, with most of the wells requiring techniques such as maintaining pressure or using an artificial lift to produce oil or gas effectively. During a well's life, the techniques used are changed to suit the changing conditions of the well, and different methods can sometimes be combined simultaneously. Production Optimization activities include but are not limited to [3]:

- Near-wellbore profile management – e.g., near-wellbore conformance management.
- Removal of near-wellbore damage – e.g., matrix stimulation.
- Maximizing the productivity index – e.g., the application of hydraulic fracturing.
- Well integrity – e.g., casing and cement failure prevention and repair.

Different mechanisms are used to recover specific percentages of the oil. Fig. 1 shows the various types of oil recovery, as defined by the Society of Petroleum Engineers, and their corresponding recovery factors. Conventional recovery (primary and secondary recovery) targets the mobile oil in the reservoir, while tertiary recovery, or enhanced oil recovery (EOR), targets the immobile oil [4].

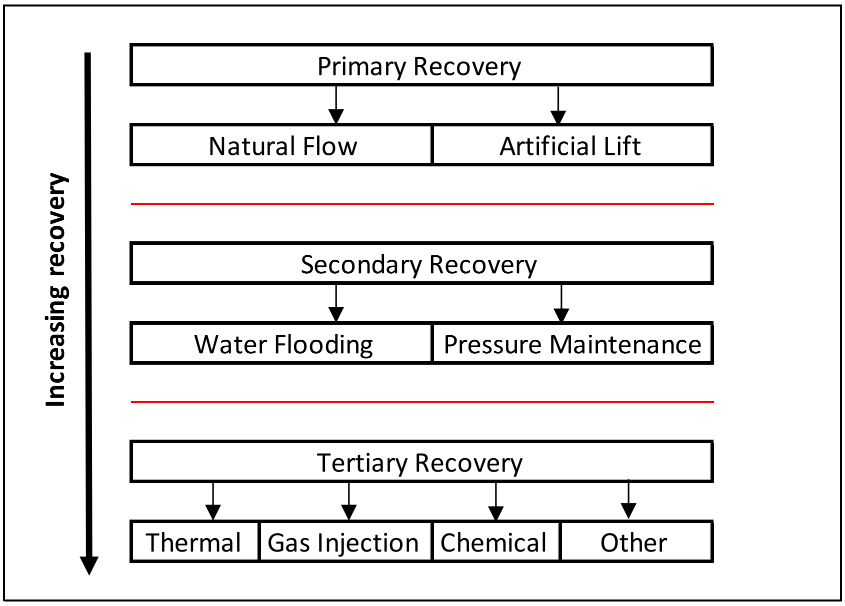

Figure 1. Various stages of oil recovery and the corresponding oil recovery factor (Adopted from [4])

Drive mechanisms play a big part in a field's or well's optimization. Some primary drive mechanisms include expansion drive, water drive, gravity drainage system, and compaction drive. The water drive method is very effective, with recovery factors averaging 40 % and ranging from 35 % to more than 75 % [5]. While some fields (typically shallow reservoirs) quickly deplete in pressure, others can have enough pressure to produce for years before any optimization techniques are required. In some cases, reservoirs may have a robust aquifer (water drive mechanism) that can support and maintain pressure during the production of the hydrocarbons; as a result, there will not be a need for interventions like waterflooding or pressure maintenance because it happens naturally. Therefore, reservoirs with subpar primary drives have a good chance of flooding.

Overview of Waterflooding

In secondary recovery, water or gas is injected into the reservoir to produce more oil or gas by increasing a well's production rate following the primary drive's inability to provide sufficient pressure to produce the hydrocarbons (see Fig. 2). In theory; the water is expected to replace produced hydrocarbons, so maintaining reservoir pressure, while sweeping unproduced hydrocarbons towards the wellbore. Waterflooding is the most commonly utilized in fluid injection procedures because water is readily available, easy to inject, and can move through the pay zone due to its efficiency in displacing oil [6].

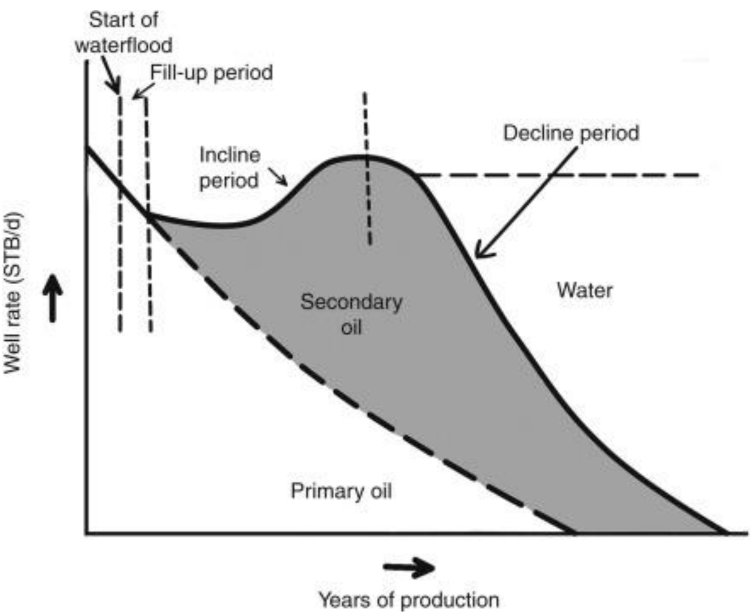

Figure 2. Waterflooding (secondary recovery) recovers a significant amount of oil, as shown by the shaded portion [7]

The efficiency of this procedure varies according to several parameters, such as oil viscosity, the mineralogical makeup of the rock present in the reservoir, recovery potential, sweep efficiency, water injectivity, and rock stability, to mention a few [8]. However, some factors need to be considered before opting for waterflooding [7]:

1. Reservoir geometry: the geometry of a reservoir plays a significant part in the design of the ideal water injection method which can be used on the reservoir. A reservoir with a water drive is commonly not subjected to water injection practices.
2. Reservoir depth: significantly influences the technical and economic aspects of the operations.
3. Fluid properties: for example, the viscosity of the oil influences the mobility ratio, which is an important property to consider when considering waterflooding because it controls the sweep efficiency.
4. Lithology and rock properties: flooding effectiveness is determined by rock properties such as clay percentage, formation thickness, porosity, and permeability.

Waterflooding aims to help the oil move forward to the producing well; that is, water should sweep the oil from the injecting well to the producing well. The complication is that the reservoir is usually not homogenous, with varying formation properties across different regions. So, because water always chooses the area with the least resistance, it is possible that the injected water will not improve oil production. However, when designing for waterflooding, well spacing, waterflooding patterns, lithology, and reservoir-fluid properties must be critically considered [9]. The first step in ensuring a successful project is to select the best waterflooding pattern [10]. The idea behind choosing the best pattern is to maximize oil contact with the injection fluid in the reservoir. Following the design pattern, producing wells can be converted into injection wells, or new wells can be drilled in the field. The number of existing wells and their location significantly influence the flood pattern that can be used. Four types of well patterns are used in fluid injection projects [11]:

1. Regular injection patterns: a consecutive repetition in a specific geometrical arrangement of wells.
2. Peripheral injection patterns: oil is displaced towards the inner wells of the reservoir because the injection wells are injecting fluids at the external boundary of the reservoir.
3. Irregular injection patterns: each injection could be different from another within the affected regions.
4. Crestal and basal injection patterns: the injection occurs through wells at the top of the structure.

Considering the most common type patterns are from the regular-type group [13], the current study ignores further mention of peripheral, irregular, crestal, and basal injection patterns. The following are the most common regular-type patterns, as shown in Fig. 3:

- Direct line drive: the injection and production lines are directly opposite.

- Staggered line drive: the wells are in the same lines as the direct line, but the injectors and producers are laterally displaced by a factor of two.
    - Four spot.
    - Five spot.
    - Seven spot.
    - Nine spot.

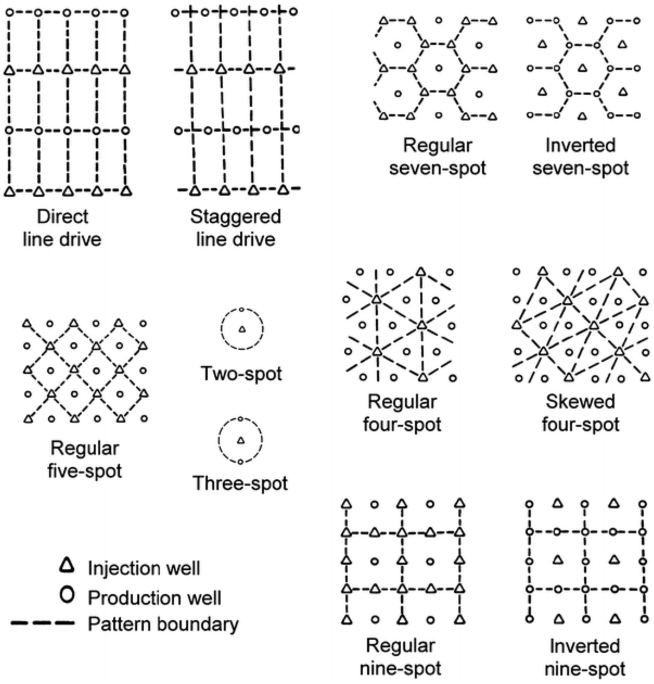

Figure 3. Well patterns commonly used in field development with injection wells for waterflooding [12]

Methodology

To analyze the effects of production optimization on oil exploration, an oil optimization simulation software is used (Modelling and simulation using Computer Modelling Group Ltd.'s technology, abbreviated as CMG)

Oil optimization modeling and simulation

Fig. 4 shows the process layout for the developed enhanced oil simulation process model.

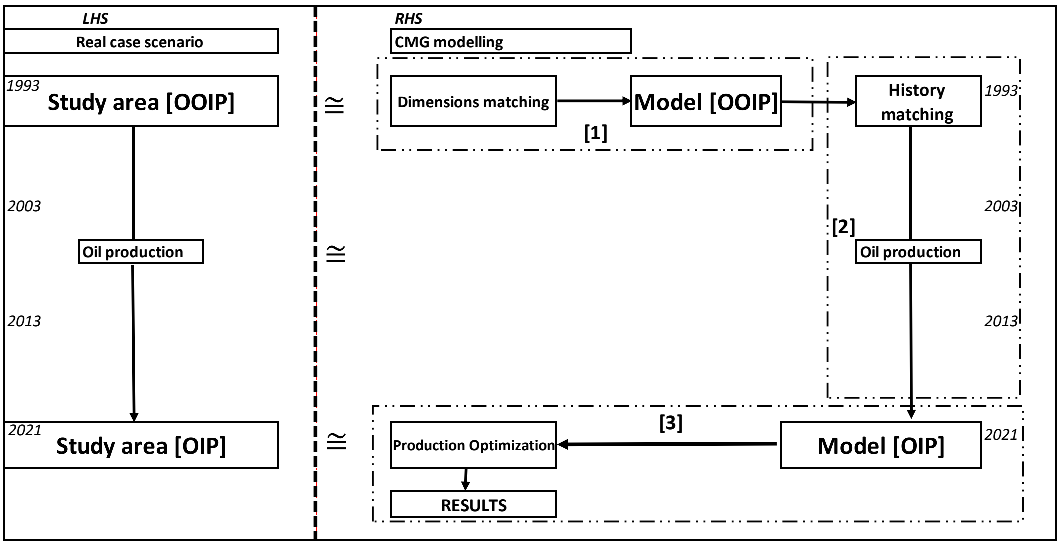

Figure 4. Methodology

The simulation is grouped into three steps, as shown in Fig. 4:

[1.] Matching the dimensions of the reservoirs (Draugen's and Model's dimensions) to match the OOIP of the Draugen field (LHS of Fig. 4), such that in 1993 the resources at the LHS are approximately equal to the resources at the RHS in Fig. 4.

   a. CMG Imex reservoir simulator is used to recreate the reservoir by dimensions matching. The simulation began by building grid blocks to match the gross volume of the Draugen field. The dimensions are as follows:

      i. i direction total distance= (80 blocks * 105 m)/1000 = 8.2 km.

      ii. j direction total distance= (40 blocks * 105 m)/1000 = 4.1 km.

      iii. k direction total distance= (1 block* 29 m)/1000 = 0.029 km.

   b. The gross volume from the simulation model is found to be 974.98 MM m^3, which is approximately equal to Draugen's gross volume of 956 MM m^3.

   c. An aquifer is added to the bottom of the reservoir to match the water influx in the Draugen field.

[2.] Adjustment of the reservoir model until it approximately reproduces the past behavior of the Draugen field reservoir. 20 production wells and 6 injection wells are drilled (according to Table 2) in the simulation to match the production at Draugen field.

   a. The production simulation is set to start on October 1, 1993, when Draugen field started its production. The following steps are carried out to match the status of the Draugen field as of 2021, when production was paused:

      i. Oil production is simulated until 2021.

      ii. 6 water injection wells are drilled for pressure maintenance.

      iii. Production optimization analysis.

[3.] Production optimization analysis of the oil saturation maps obtained from step [2.] after completing history matching. To complete the optimization, the following tasks are performed:

   a. Cutting off regions produces more water than hydrocarbons.

   b. Select the most preferred locations for new production wells to increase oil production.

      i. The field is divided into sections to assess the production of how each section performs.

      ii. The assignment of producing wells to each section.

      iii. Lastly, optimization is performed for the preferred section/sections.

Study area- Draugen field

The Draugen field is an oil field located in blocks 6407/9 and 6407/12, and the platform is located at 64.35 degrees North and 7.77 degrees East in the Norwegian Sea, as shown in Fig. 5 [13].

Figure 5. Location of Draugen field [14]

The Draugen field's wild cat well was drilled to a total depth of 2 500 m in the Late Triassic Red Beds using the semi-submersible installation and confirmed the presence of oil in the 1980s [15]. The field was expanded to include a platform and subsea wells to produce substantial oil. Oil production began in 1993 and increased until 1999, as shown in Fig. 6. From 2001, the field started producing gas and natural gas liquids, with a decrease and increase in oil and water, respectively [16]. Fig. 6 shows the oil production chart belonging to the Draugen field from 1993 to 2021.

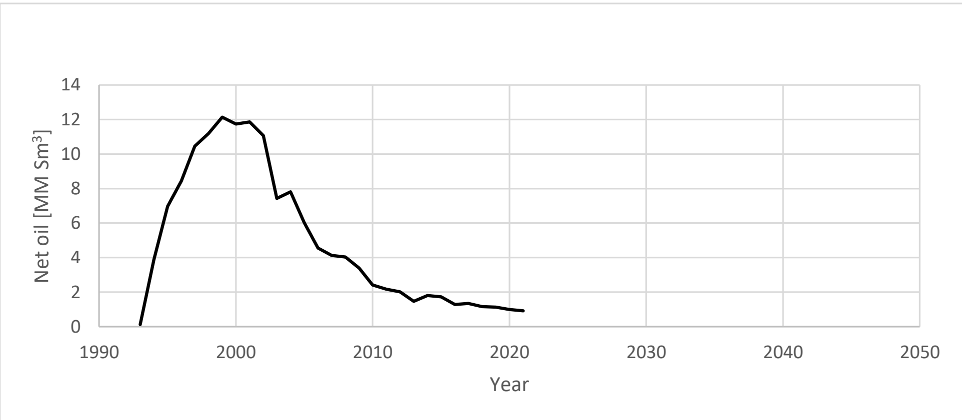

Figure 6. Oil production at Draugen field per year [16]

Table 1 shows the reservoir characteristics of the Draugen field.

Table 1. Draugen Reservoir characteristics [17]

Characteristic	
Orig. inplace oil [MM Sm^3]	227.75
Orig. recoverable oil [MM Sm^3]	151.92
Remaining oil [MM Sm^3]	8.26
Reservoir depth [m]	1 596
Oil saturation [%]	72 – 85
Porosity [%]	32
Gross reservoir thickness [m]	0 – 46 (average-29)
Oil column [m]	0 – 37
Anticline structure [km]	6 wide, 21 long
Solution oil-gas ratio [SCF/STB]	52
Oil-water contact [m]	1 638
Oil density [kg/m^3]	824
Oil viscosity [cp]	0.68
Formation volume factor [RB/STB]	1.19
Average permeability [D]	0.5
Horizontal permeability [D]	6 – 7
Clay content [%]	< 10
Average water saturation [%]	25
Initial reservoir temperature [°C]	71
Initial reservoir pressure [bar]	169
Bubble point pressure [bar]	59
Reservoir area [km^2]	60
Gross rock volume [m^3]	956 000 000
Reservoir type	The sandstone of the Late Jurassic age
Status	Declining oil production and volumes of associated gas are not sufficient for power generation

As of 2021, 31 wells directly related to production were drilled, consisting of 19 production wells, 6 injection wells, and 6 observation wells. As indicated by the decline in Fig. 6, the produced hydrocarbons are insufficient to meet the power demand. So, solutions must be devised to enhance oil and gas production.

Table 2 below shows the development of the active wells for Draugen field.

Table 2. Draugen's exploration wellbore [16]

Wellbore name	Entered date	Completed date	Purpose	Content
6407/9-11	19.10.2019	29.10.2019	Observation	Oil
6407/9-A-1	07.03.1994	12.05.1994	Production	Oil
6407/9-A-2	19.09.1994	31.10.1994	Observation	Not applicable
6407/9-A-2 A	05.11.1994	24.11.1994	Production	Oil
6407/9-A-3	11.11.1995	15.12.1995	Production	Oil
6407/9-A-4	03.06.1999	08.08.1999	Observation	Not applicable
6407/9-A-4 A	11.08.1999	02.10.1999	Production	Oil
6407/9-A-5	21.09.1995	01.11.1995	Production	Oil
6407/9-A-6	29.05.1994	18.07.1994	Production	Oil
6407/9-A-53 H	05.04.1993	08.11.1993	Production	Oil
6407/9-A-55 H	08.04.1993	26.04.1993	Observation	Not applicable
6407/9-A-55 AH	26.04.1993	11.05.1993	Production	Oil
6407/9-A-58 H	09.06.1993	23.06.1993	Injection	Gas
6407/9-B-1 H	10.08.1993	23.08.1993	Injection	Water
6407/9-B-2 H	19.07.1993	08.04.1994	Injection	Water
6407/9-B-5 H	27.07.1993	27.04.1994	Injection	Water
6407/9-C-1 H	27.09.1993	12.12.1993	Injection	Water
6407/9-C-2 H	15.10.1993	27.12.1993	Injection	Water
6407/9-D-1 H	23.05.2001	30.05.2001	Observation	Not applicable
6407/9-D-1 AH	31.05.2001	02.07.2001	Production	Oil
6407/9-D-2 H	08.06.2001	18.06.2001	Production	Oil
6407/9-D-3 H	14.02.2008	22.03.2008	Production	Oil
6407/9-E-2 H	09.05.2002	10.06.2002	Production	Oil
6407/9-E-3 H	22.11.2007	04.01.2008	Production	Oil
6407/9-E-4 H	11.06.2013	29.09.2013	Production	Oil
6407/9-F-1 H	11.06.2003	23.06.2003	Observation	Not applicable
6407/9-G-1 H	11.05.2014	30.05.2014	Production	Oil
6407/9-G-2 H	08.07.2014	23.07.2014	Production	Oil
6407/9-G-3 H	11.06.2014	25.06.2014	Production	Oil
6407/9-G-5 H	11.06.2015	08.07.2015	Production	Oil

Results

Dimensions matching results

Following the first step from the methodology in Fig. 4, Fig. 7 shows the models with dimensions approximately equal to the dimensions of the Draugen field. The reservoir simulation model has a total gross volume of 974.98 MM m^3, comparable to the actual gross volume of the field, which is 956 MM m^3. An aquifer was added to the reservoir's bottom to match the water influx in the actual reservoir. The compressibility of the reservoir rock was set to 5.8E-07 1/psi. Fig. 7 (a) shows the 3D view of the reservoir generated using CMG, whereas, Fig. 7 (b) shows the location of 20 production and 6 injection wells.

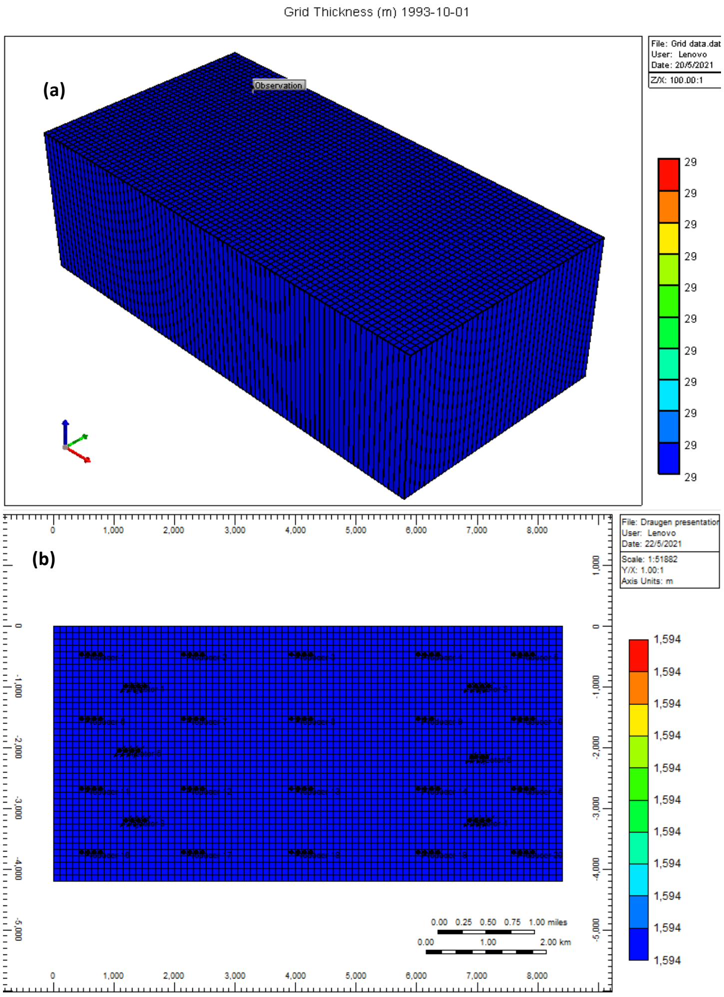

Figure 7. Model dimensions used in the CMG model

To maximize oil production throughout the field, 20 producing wells were evenly distributed throughout the reservoir. The well constraints in the model were tailored to match the Draugen field's production history. The field used six injection wells to provide pressure support and help push oil from the reservoir to the producing wells. The bubble point pressure was never reached because the reservoir pressure was relatively high compared to the bubble point pressure, which was ideal for ensuring that the gas did not evolve out of the oil, potentially affecting the oil's production rates.

History match results

To show the CMG results from the history match, Fig. 8 shows the oil saturation map, 13 years from 1993, while Fig. 9 shows the yearly field simulation of oil and water from 1993 until 2021 when production was stopped at Draugen field.

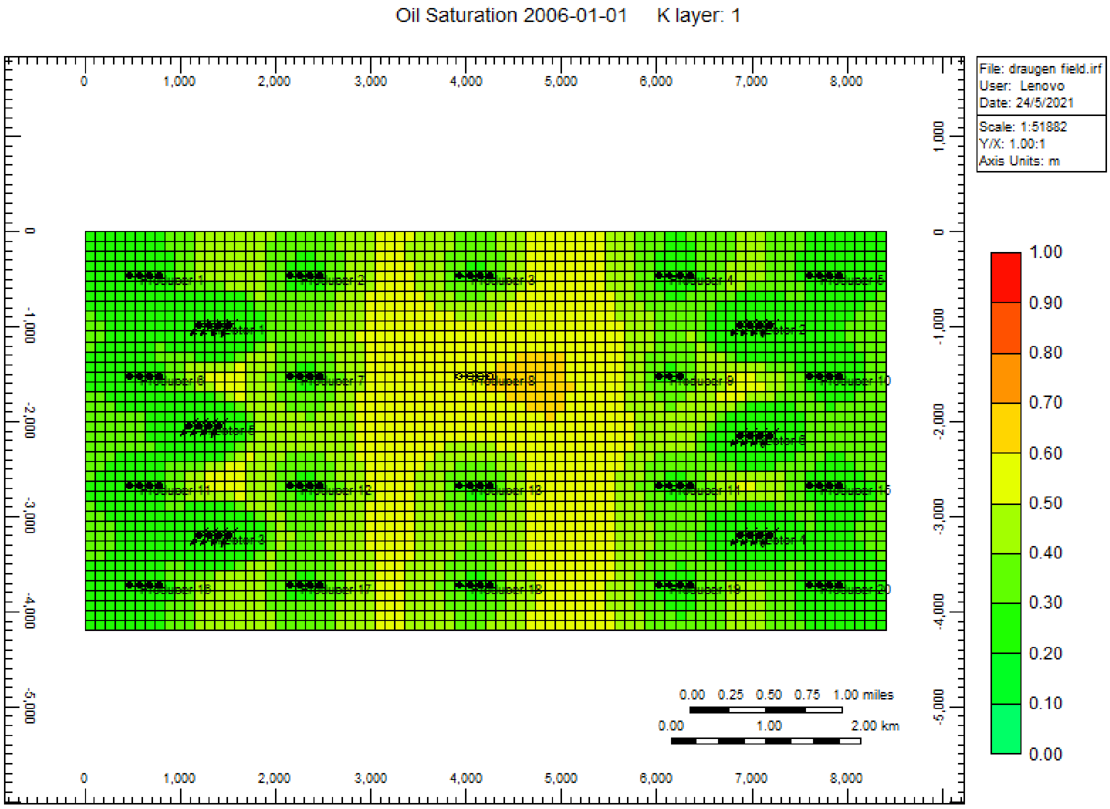

Figure 8. Oil saturation map simulation model

As shown in Figs. 8 and 9, the map of the remaining oil in place is critical for deciding how and where to optimize the production data, as oil production decreased when more water was produced in 2005. Water production exceeded oil production from 2005 to 2021. On May 1, 2021, the oil production was 649 288 m^3, while the water yield was 3 000 130 m^3.

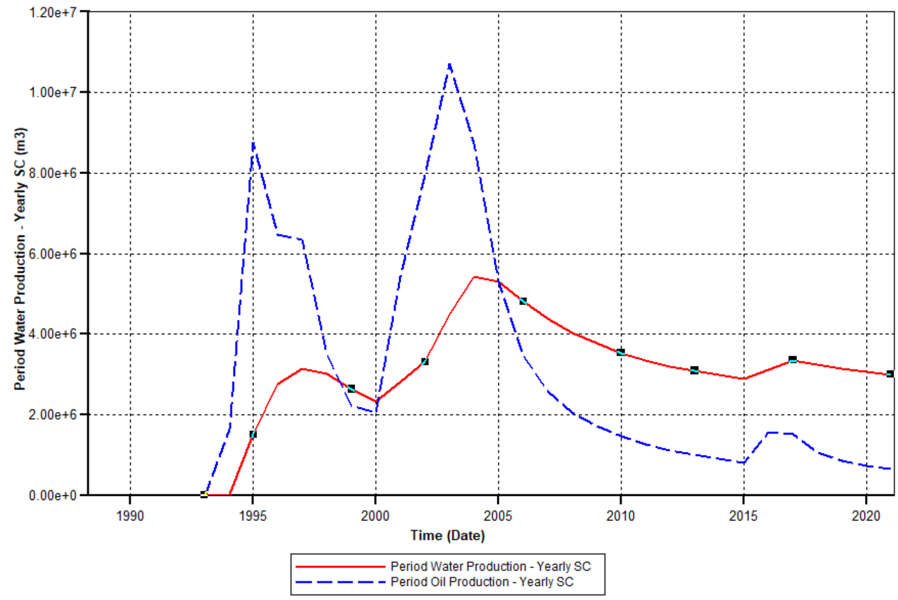

Figure 9. Yearly field simulation of oil and water from 1993 until 2021

Fig. 10 shows the oil saturation map in 2021, after completing a successful history match.

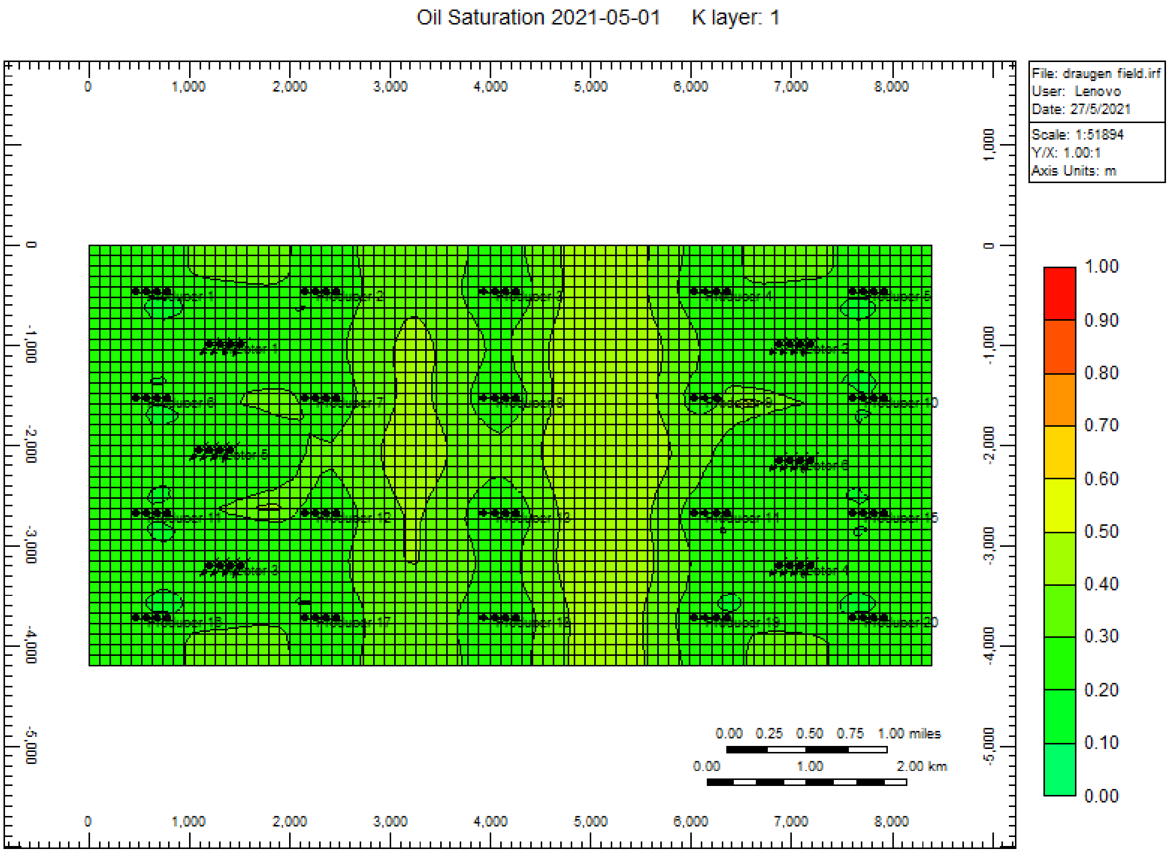

Figure 10. Oil saturation map simulation model in 2021

Production optimization analysis results

The field was divided into 5 sections to evaluate how well each section performed in production throughout the simulation. Each section contains 4 producing wells. The results are depicted in Fig. 11. Sections 1 and 5 began producing earlier in the reservoir's life, causing oil saturation to fall faster than the other sections. The 6 injection wells were also placed within these sections to provide pressure support and waterflooding, which increased the production of oil in the more centrally located sections. As a result, the oil saturation reached 23.5% in Sections 1 and 5 on May 1, 2021, which is close to the residual oil saturation.

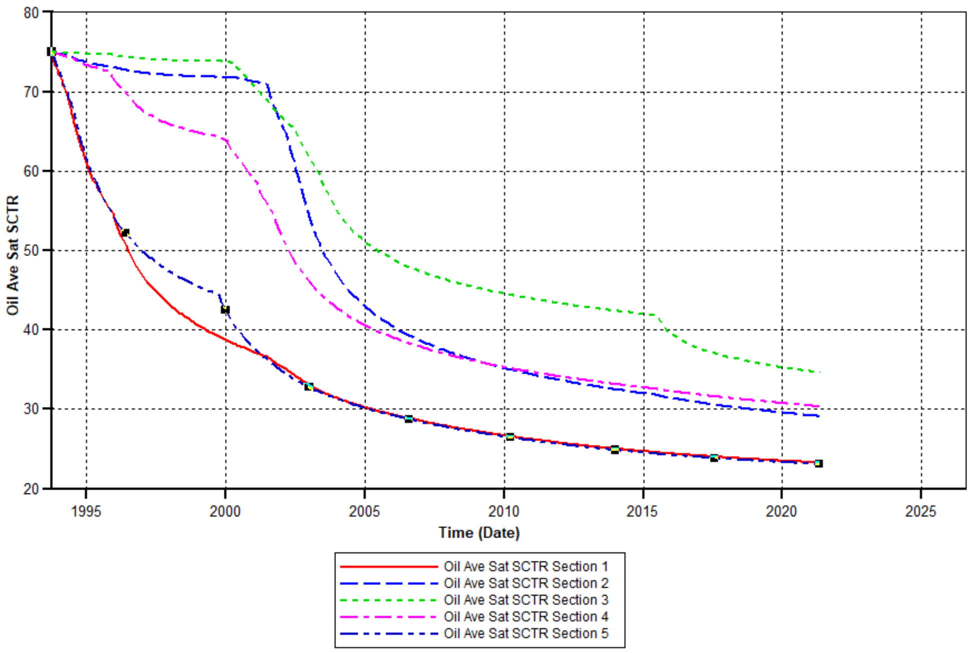

Figure 11. Oil saturation of the sections belonging to Draugen's simulation model

Sections 1 and 2 had the highest water saturation of about 74% as of May 1, 2021, according to the water saturation plot in Fig. 12. This suggests that these areas contribute a significant amount of water.

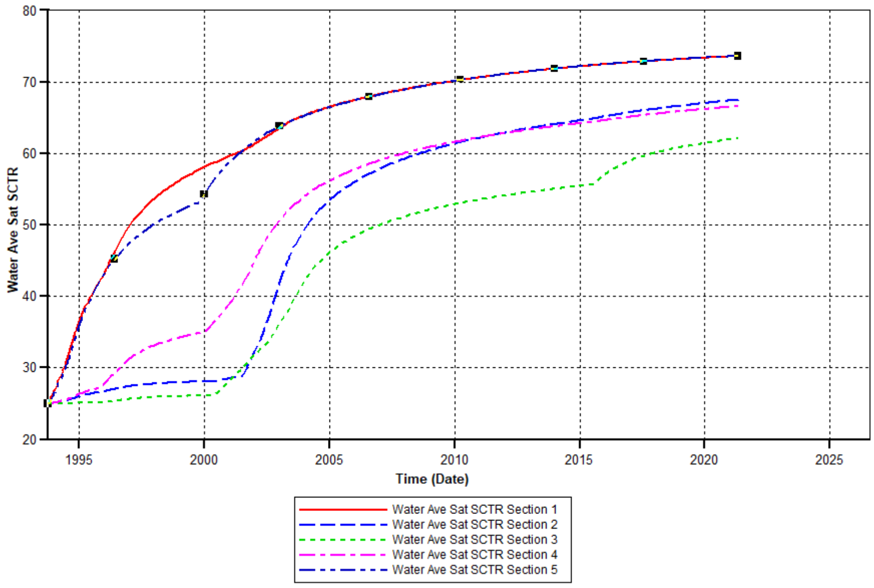

Figure 12. Water saturation of the 5 sections belonging to Draugen's model

After careful analysis of Figs. 9,10, 11, and 12, the following recommendations were made to improve the field oil production:

1. Shut in the producing wells in Sections 1 and 5.
2. Shut all the present injection wells in the field.
3. Allow production to continue in Sections 2, 3, and 4 till oil saturation reaches residual oil saturation.
4. Complete new production wells located in the regions with high oil saturation to increase oil production.
5. Complete new injection wells using a regular-type pattern in a strategic placement to recover more hydrocarbons from the field efficiently.

Accordingly, additional 4 producing wells were completed and placed in regions with the highest oil saturation (see Fig. 10). The ideal locations for the new producing wells were determined to be blocks 48,11,1, 48,31,1, 28,11,1, and 28,31,1. Also, 2 injection wells were completed, and each was located between 2 new producing wells in blocks 48,20,1 and 28,20,1.

As shown in Fig. 13, the production optimization increased the oil production from 649 288 m^3 on May 1, 2021, to a peak of 3 408 230 m^3 by January 2022. However, water production also increased because of the water invasion from the aquifer. The production gradually decreased until all sections reached residual oil saturation, as in Fig. 14, production was complete from the reservoir, and all the wells were shut-in. Fig. 15 shows the cumulative production obtained after the simulation run was completed in 2050.

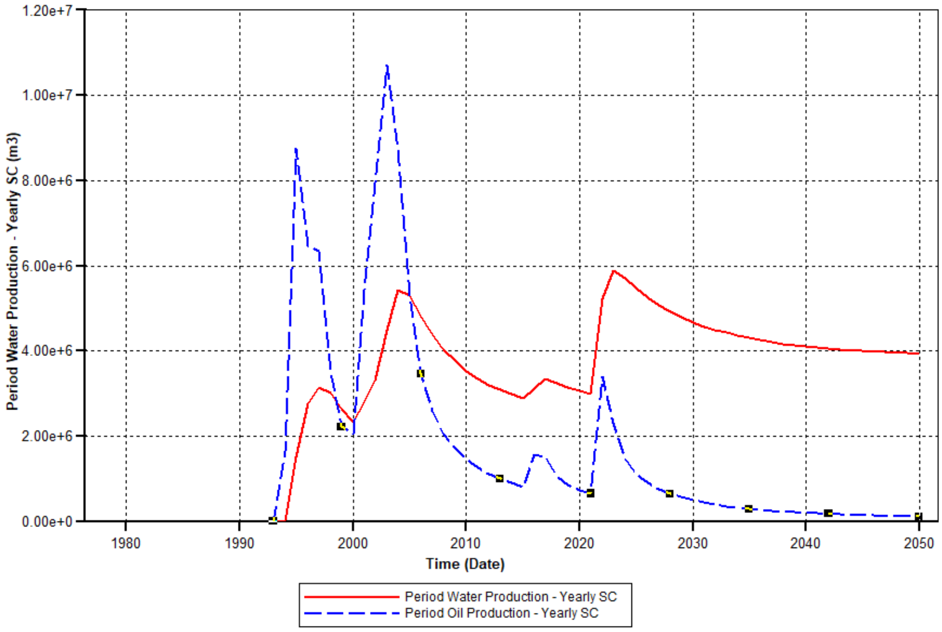

Figure 13. Oil and water production after optimization

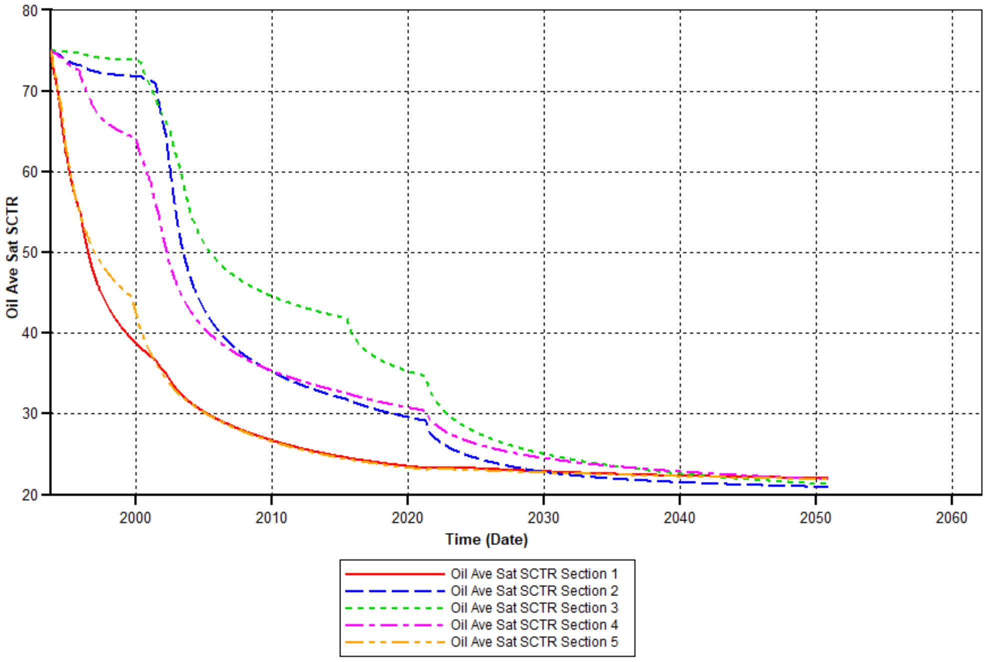

Figure 14. Oil saturation after optimization

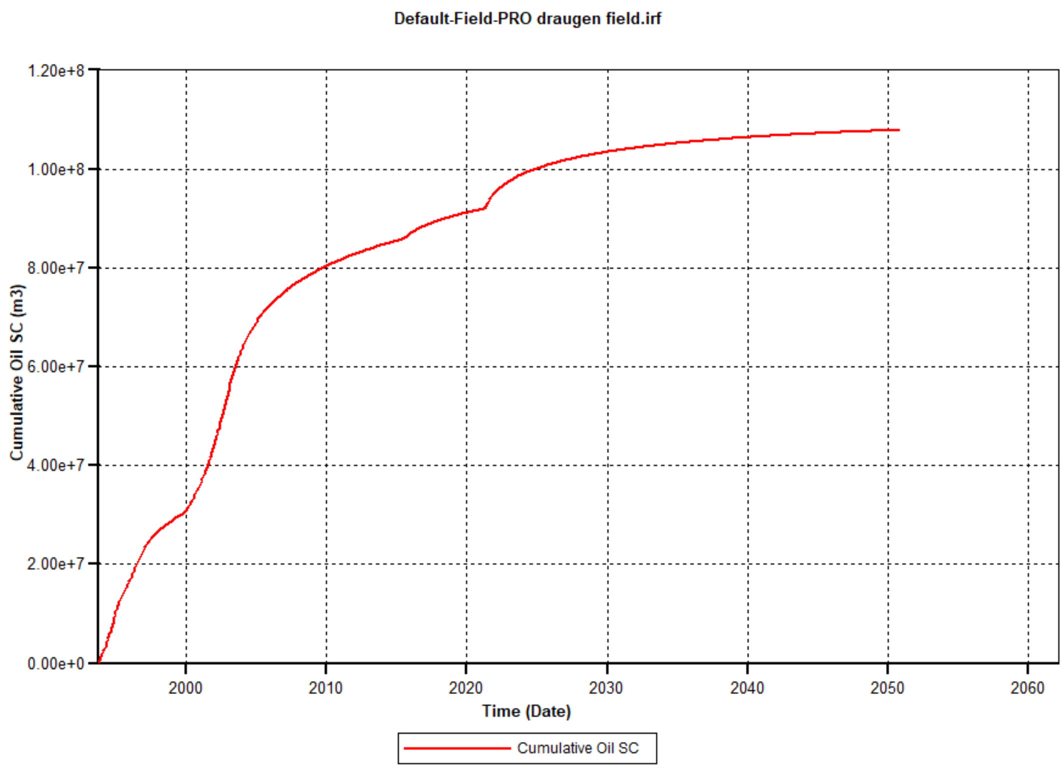

Figure 15. Cumulative oil production from 1993 until 2050

There is a notable increase in production from 2021 owing to the waterflood (which increases the reservoir pressure, as shown in Fig. 16) and new production wells added, as shown in Fig. 17.

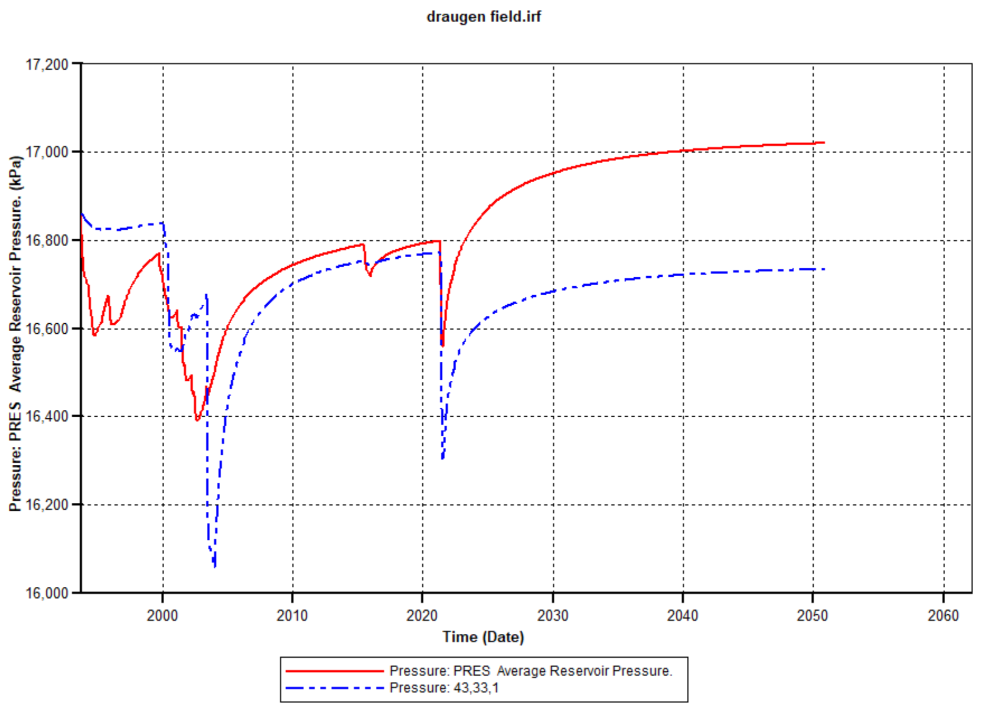

Figure 16. The average pressure of the entire field

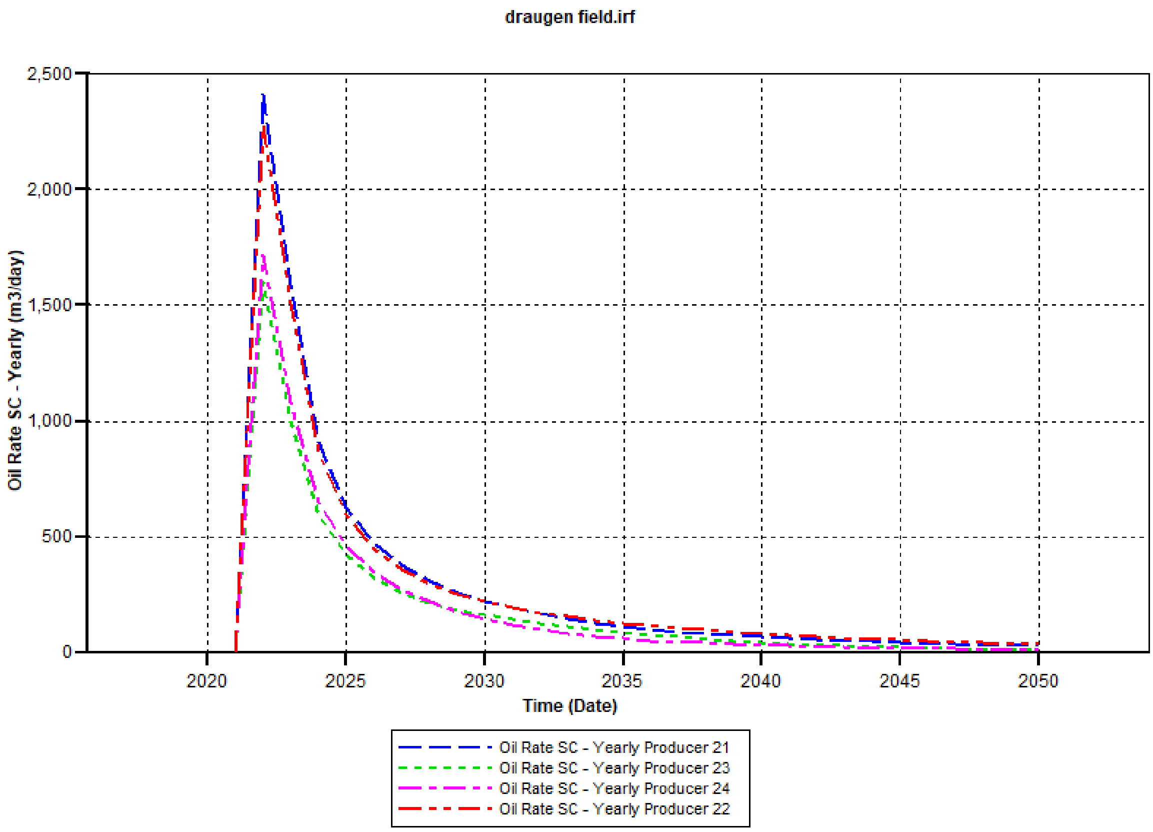

Figure 17. Decline curves of the new wells

Conclusion

The current study was conducted with the following conclusions:

- Total shutdown and discontinuation of production from Sections 1 and 5 because the sections had no noticeable impact on cumulative oil production. Sections 1 and 5 were incompetent because they had reached residual oil saturation.
- Adding 4 production and 2 injection wells proved to be successful in optimizing oil production, which increased from 649 288 m^3 on May 1 2021, to a peak of 3 408 230 m^3 by January 2022.
- At the end of the simulation, the entire reservoir had an average oil saturation of 23 %, approximately equal to the field's residual oil saturation.
- The cumulative oil production was increased from a projected 99 500 000 m^3 before optimization to 108 370 000 m^3 after optimization.
- Accordingly, the results effectively support the optimization of oil production via waterflooding.

Moreso, it is possible to reduce oil saturation from 23 % to lower saturations by applying chemical flooding. However, a feasibility assessment involving core sampling and additional petrophysical studies must be conducted before applying the technology.

Declaration of Competing Interest Statement.

The authors declare that they have no known competing financial interests or personal relationships to influence the work reported in this paper.

Credit Authorship Contribution Statement.

Tendai Zisengwe: Conceptualization, Methodology, Software, Formal analysis, Resources, Project administration.

Bruce Mutume: Validation, Resources, Writing - Original Draft, Writing - Review & Editing, Visualization, Supervision.

Author Biographies.

Tendai Zisengwe, MSc is a graduate in Petroleum and Natural Gas Engineering at Near East University. Research interests include oil and gas engineering, oil and gas secondary recovery methods.

Bruce Mutume, MSc is a graduate in Sustainable Environment and Energy Systems at Middle East Technical University. Research interests include resource estimation and production, oil and gas production optimization, hybrid power technology, and sustainable energy.

Funding: This research did not receive any specific grant from funding agencies in the public, commercial, or not-for-profit sectors.

Acknowledgements.

Authors acknowledge use of library and IT resources of Middle East Technical University Northern Cyprus Campus and of Near East University.

References

[1] Fayaed SS, El-Shafie A, Jaafar O. Reservoir-system simulation and optimization techniques. Stoch Environ Res Risk Assess 2013;27:1751–72. https://doi.org/10.1007/s00477-013-0711-4.

[2] Ashena R, Bataee M, Jafarpour H, Abbasi H, Zolotukhin A, Mirhashemi M. Significant production improvement using optimization of completion and artificial lift: case studies from South-West Iran. J Pet Explor Prod 2021;11:359–84. https://doi.org/10.1007/s13202-020-01053-6.

[3] Petroleum Production Optimization. OilGas Portal n.d. https://www.oil-gasportal.com/petroleum-production-optimization/ (accessed February 14, 2023).

[4] Kokal S, Al-Kaabi A. Enhanced oil recovery: challenges & opportunities. Environ Sustain n.d.

[5] Rui Z, Lu J, Zhang Z, Guo R, Ling K, Zhang R, et al. A quantitative oil and gas reservoir evaluation system for development. J Nat Gas Sci Eng 2017;42:31–9. https://doi.org/10.1016/j.jngse.2017.02.026.

[6] C CF. The Reservoir Engineering Aspects of Waterflooding. Monogr Ser Soc Pet Eng AIME 1971.

[7] Satter A, Iqbal GM. 16 - Waterflooding and waterflood surveillance. In: Satter A, Iqbal GM, editors. Reserv. Eng., Boston: Gulf Professional Publishing; 2016, p. 289–312. https://doi.org/10.1016/B978-0-12-800219-3.00016-4.

[8] Hermansen H, Landa GH, Sylte JE, Thomas LK. Experiences after 10 years of waterflooding the Ekofisk Field, Norway. J Pet Sci Eng 2000;26:11–8. https://doi.org/10.1016/S0920-4105(00)00016-4.

[9] Rose SC, Buckwatter JF, Woodhall RJ. The design engineering aspects of waterflooding 1989.

[10] Ahmed T. Chapter 14 - Principles of Waterflooding. In: Ahmed T, editor. Reserv. Eng. Handb. Fourth Ed., Boston: Gulf Professional Publishing; 2010, p. 909–1095. https://doi.org/10.1016/B978-1-85617-803-7.50022-5.

[11] Reservoir Engineering Handbook - 4th Edition n.d. https://www.elsevier.com/books/reservoir-engineering-handbook/ahmed/978-1-85617-803-7 (accessed February 15, 2023).

[12] Weijermars R, van Harmelen A. Advancement of sweep zones in waterflooding: conceptual insight based on flow visualizations of oil-withdrawal contours and waterflood time-of-flight contours using complex potentials. J Pet Explor Prod Technol 2017;7:785–812. https://doi.org/10.1007/s13202-016-0294-y.

[13] Gudmestad OT. Modelling of Waves for the Design of Offshore Structures. J Mar Sci Eng 2020;8:293. https://doi.org/10.3390/jmse8040293.

[14] New PG. Chevron sells stake in Draugen to VNG. Petro Glob News 2014. https://petroglobalnews.com/2014/06/chevron-sells-stake-in-draugen-to-vng/ (accessed February 12, 2023).

[15] Kvaal M, Henriksen B, Sorenes T. The Economics of Exploration On the Norwegian Continental Shelf, OnePetro; 2005.

[16] Field: DRAUGEN - Factpages - NPD n.d. https://factpages.npd.no/en/field/pageview/all/43758 (accessed February 12, 2023).

[17] Faktasider - OD n.d. https://factpages.npd.no/en/wellbore/PageView (accessed February 12, 2023).